Lawrence Berkeley National Laboratory

Title

Validation of an inverse model of zone air heat balance

Permalink

https://escholarship.org/uc/item/6093p9mw

Authors

Lee, Sang Hoon
Hong, Tianzhen

Publication Date

2019-08-01

DOI

Peer reviewed

Validation of An Inverse Model of Zone Air Heat Balance

Sang Hoon Lee, Tianzhen Hong[*]

Building Technology and Urban Systems Division

Lawrence Berkeley National Laboratory, United States, USA

*Corresponding author: T. Hong, 1(510)486-7082, thong@lbl.gov

Abstract

This paper presents the validation method and results of an inverse model of zone air heat balance. The inverse model, implemented in EnergyPlus and published in a previous article [1], calculates highly uncertain model parameters such as internal thermal mass and infiltration airflow by inversely solving the zone air heat balance equation using the easy-to-measure zone air temperature data. The paper provides technical details of validation from the experiments using LBNL's Facility for Low Energy eXperiment in Buildings (FLEXLAB) that measures zone air temperature under the controlled experiment of two levels of internal mass and four levels of infiltration airflow. The simulation results of the zone infiltration airflow and internal thermal mass from the inverse model agree well with the measured data from the FLEXLAB experiments. The validated inverse model in EnergyPlus can be used to enhance the energy modeling of existing buildings that enables energy performance assessments for energy efficiency improvements.

1. Introduction

Buildings in the United States consume 40% of primary energy. It is critical to reducing energy use in the building sector through improving their operations or retrofitting with energy-efficient technologies, which supports the energy and environmental goals of federal, state and local governments. Retrofit of existing buildings offers an opportunity to improve building energy performance. Building simulation has been widely used as a powerful tool to support the design of new buildings and evaluate retrofit measures for existing buildings. However, there is a challenge in simulating the energy performance of existing buildings, because model inputs that have significant impacts on simulation results may be unknown or have high uncertainty. There are various energy modeling methods covering a wide spectrum of model fidelity, including the detailed physics-based dynamic simulations [2–4], reduced-order models [5–7], and data-driven statistical methods [8–10], which offer many building energy performance analysis applications [11,12]. High-fidelity physics-based dynamic simulations can offer the most accurate energy performance analysis. However, drawbacks are they require a significant number of building parameters as input, and some of them are difficult to obtain in practice. Moreover, some input parameters are highly unknown and hard to measure, leading to large uncertainty in energy saving estimates [12–15].

An inverse modeling approach, that can help reduce these uncertainties, was introduced in a previous article [1]. The inverse model calculates highly

uncertain input parameters such as internal thermal mass and infiltration airflow with easily measurable zone air temperature data. The inverse modeling approach takes advantage of the more widely available data streams from IoT devices such as smart thermostats in buildings. Thermal mass plays a key role in the transient behavior and thermal inertia of a building [16]. Many of energy modeling applications take into account the thermal inertia of the envelope and the floors more importantly. However, internal thermal mass related inputs such as furniture, partitions, and books have not been treated well in building energy simulation. Typically internal zones are treated as an empty space filled with air only in energy models [17–19]. Zone air infiltration airflow is another important input that has significant impacts on the cooling and heating energy demand [20]. The infiltration airflow is dynamically influenced by the indoor and outdoor climatic conditions. Infiltration is difficult to measure and characterize. Blower door testing is usually applied to residential buildings while hard for commercial buildings. Specifying the sizes and distribution of cracks in the building envelope, the permeability of the envelope, the airflow to the building, and the pressure distribution in and around the building is impractical [21]. Difficulties in measuring internal thermal mass and infiltration airflow rates contribute to the uncertainty of simulated results, which hinders an accurate estimate of energy savings in retrofit projects.

The inverse modeling approach derives physical characteristics of the internal thermal mass and infiltration by inversely solving the zone air heat

balance equations using the measured zone air temperatures, which renders solutions as alternatives to direct measurements from the use of inverse modeling techniques [22]. This inverse model was implemented in EnergyPlus version 8.7 and details of inverse model algorithms were introduced in [1]. EnergyPlus is DOE's open source building energy simulation engine that enables a whole building energy performance analysis for engineers, architects, and researchers [23] and enables testing of new features, which makes it ideal for the implementation and verification of the inverse models.

Using EnergyPlus, the internal thermal mass can be modeled in two approaches. One way is to use EnergyPlus input object, *InternalMass*, which enables specifying construction materials and their surface areas. The *Internalmass* object participates in the zone air heat balance and the longwave radiant exchange. The geometry of the internal mass construction is greatly simplified due to the difficulty of measurement. They do not directly interact with the solar heat gain because the internal mass objects do not have a specific location in space. Internal mass objects can represent multiple pieces of interior mass (furniture, partitions) with different constructions.

Alternatively, *ZoneCapacitanceMultiplier:ResearchSpecial* object can be used to sidestep challenges in determining volumes and thermal properties of individual internal thermal mass objects. Temperature capacitance multipliers from the special object can equivalently represent the effective

storage capacity of the zone internal thermal mass [4]. The default capacitance multiplier of 1.0 implies the capacitance comes only from the air in the zone. This multiplier can be increased if the zone air capacitance needs to be increased for the stability of the simulation, which represents the actual internal thermal mass including the furniture and interior partition walls. The previous article [1] described these two internal mass modeling approaches using EnergyPlus in detail, as well as the derivation of the temperature capacitance multiplier from the inverse model.

The validation of new energy algorithms can be achieved using dynamic testing and data analysis to characterize the actual energy performance of building components and whole buildings comparing with the model outcomes [24]. Validation of the developed inverse model uses data collected from experiments conducted at the Facility for Low Energy Experiment in Buildings (FLEXLAB), a testbed for building energy efficiency research located at the Lawrence Berkeley National Lab (LBNL) [25]. FLEXLAB provides researchers a flexible facility to study energy efficiency of building systems. Eight test cells (including two high bay test cells and two rotating test cells) can test HVAC, lighting, fenestration, facade, control systems and plug loads under real-world conditions. By providing the ability to install customized systems into a test cell, FLEXLAB allows users to test the functionality and performance of a specific building configuration. FLEXLAB experiments offer a better understanding of real-world performance than can be achieved through simulation alone. FLEXLAB customization

options include building systems such as lighting, HVAC and controls and architectural elements including external shading, fenestration, interior shading, ceiling, floors, furniture, and finishes [26]. FLEXLAB provides a controlled, highly instrumented building technology testbed that enables assessing the indoor environment and energy savings potential under a range of conditions expected to occur in the real world [27–31]. FLEXLAB is used to support the ASHRAE 140 framework to improve characterization of building energy modeling engine accuracy and to provide a consistent validation framework that provides confidence in energy simulations [32]. The paper provides technical details of the inverse model validation using the EnergyPlus simulation and measured data from the FLEXLAB experiment.

2. FLEXLAB Experiment

LBNL's FLEXLAB enables testing of building systems individually or as an integrated system under real-world conditions for flexible, comprehensive, and advanced experiments [33,34]. The facility comprises four testbeds, each with two identical thermally isolated cells. Cells are heavily instrumented with numerous sensors and meters that monitor the performance of HVAC systems, lighting, windows, building envelope, control systems, and plug loads [35]. The validation task used FLEXLAB testbed cell 3A for 50 days from April 4 to May 23, 2016. Figure 1 shows the exterior view of the testbed, Figure 2 for the floor plan and the elevation view, and Table 1 provides details of the cell envelope.

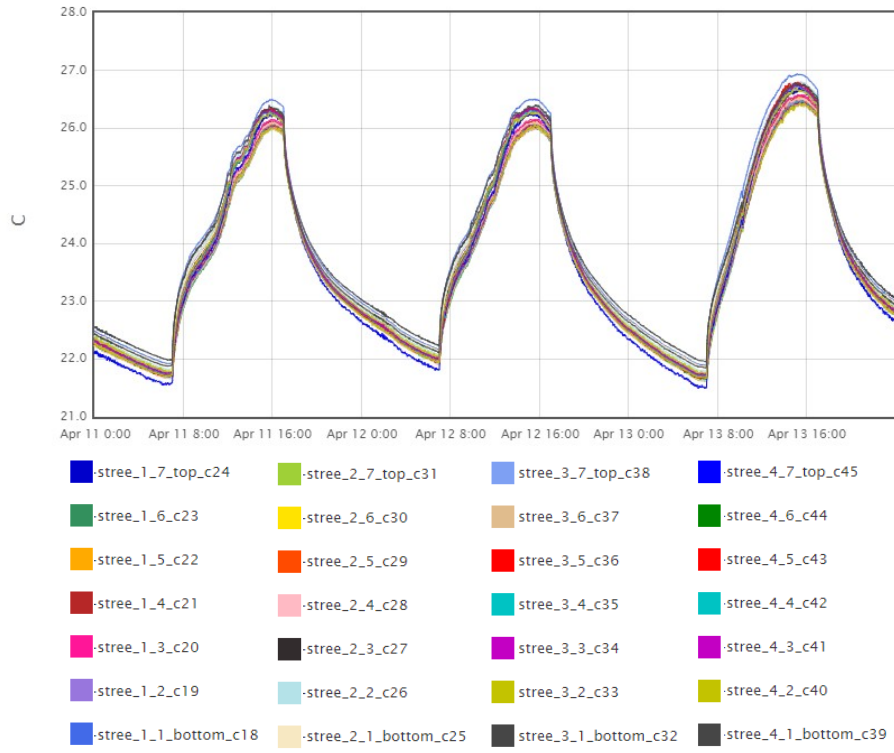Figure 1 Exterior View of the FLEXLAB Testbed Cell 3A
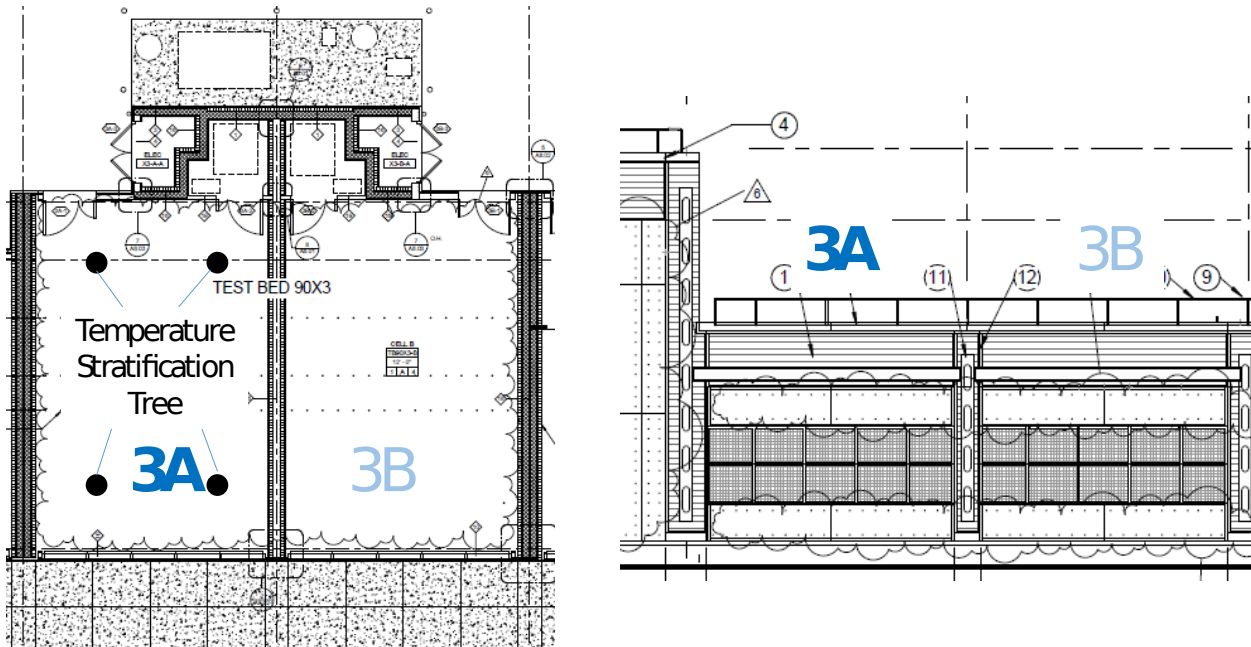
(a)

(b)

Figure 2 FLEXLAB Testbed Cell 3A Floor Plan and Elevation View

Table 1 FLEXLAB Testbed Cell 3A Envelope Specification

Depth (South-North)	30 ft (9.1 m)
Width (East-West)	21.9 ft (6.7 m)
Height (floor-ceiling)	12 ft (3.7 m)

Floor area		657 ft^2 (61 m^2)
Envelope	South, North	Metal stud with R-13 batt insulation & R-3.8 continuous rigid insulation
	East, West	Adiabatic
Glazing	South	138 ft^2 (12.8 m^2) with 10 panels (SHGC-0.25, U-0.60 BTU/(h·°F·ft^2) (3.4 W/(K·m^2))

The accurate measurement of the indoor zone air temperature under various infiltration air flow rates and internal mass configurations was the key to the experiment for the inverse model validation. Four stratification temperature sensor trees with a total of 28 temperature sensors were installed at the corner points of the test cell to measure the indoor zone air temperature. Each tree, Figure 3 (a) has seven temperature sensors placed at equal intervals from the floor to the ceiling. Temperature data were recorded at a one-minute interval and stored in an sMAP (Simple Measurement and Actuation Profile) system. Figure 3 (b) shows an example of the measured temperature data from the 28 temperature sensors for three days. Each color indicates the temperature data from each sensor, and each legend represents one of the seven temperature sensor trees to capture the stratification effect. The controlled internal heat loads were used for the experiment, which represents a typical office of 21 W/m^2 (2 W/ft^2) with the operation schedule between 8 am and 6 pm and off for other hours [36]. The air mixing fans were programmed to operate for 24 hours to ensure a well-mixing of zone air during the whole experiment. The HVAC system was turned off for the entire experiment.

■ stree_1_7_top_c24	■ stree_2_7_top_c31	■ stree_3_7_top_c38	■ stree_4_7_top_c45
■ stree_1_6_c23	■ stree_2_6_c30	■ stree_3_6_c37	■ stree_4_6_c44
■ stree_1_5_c22	■ stree_2_5_c29	■ stree_3_5_c36	■ stree_4_5_c43
■ stree_1_4_c21	■ stree_2_4_c28	■ stree_3_4_c35	■ stree_4_4_c42
■ stree_1_3_c20	■ stree_2_3_c27	■ stree_3_3_c34	■ stree_4_3_c41
■ stree_1_2_c19	■ stree_2_2_c26	■ stree_3_2_c33	■ stree_4_2_c40
■ stree_1_1_bottom_c18	■ stree_2_1_bottom_c25	■ stree_3_1_bottom_c32	■ stree_4_1_bottom_c39

(a)   (b)

Figure 3 Stratification sensor tree to measure zone air temperature

The experiment measured the air temperatures under a range of interior

environmental configurations of light and heavy internal mass and tight and

leaky air infiltration as below:

- Internal mass:
  - Light mass (IM0): represents a very light office configuration with six sets of light-mass desks, chairs, cotton manikins, desktop computers, and monitors (Figure 4)
  - Heavy mass (IM1): represents an office configuration with books (For experiment about 1000 library books in 50 boxes are added to the cell space) (Figure 5)
- Infiltration air flow rates:
  - Tight infiltration rate (INF0): 0.1 air change per hour (ACH), a natural cell condition with doors, windows, and air dampers closed
  - Medium infiltration rate (INF1): 0.4 ACH controlled with a designated exhaust fan

- High infiltration rate (INF2): 2.0 ACH controlled with a designated exhaust fan
- Infiltration with a schedule (INF3): 0.18 ACH (6 am – 10 pm) and 0.7 ACH(10 pm – 6 am) controlled with a designated exhaust fan

Infiltration levels were selected to represent typical office settings defined by ASHRAE 90.1 in terms of infiltration flow rate per surface area. To represent a poor infiltration level, ASHRAE 90.1-2004 office model is used, which has the infiltration rate of 0.00102 $m^3/s/m^2$ (surface area) [37], about 2 ACH in the FLEXLAB testbed cell. To represent a good infiltration level, ASHRAE 90.1-2016 office model is used, which has an infiltration rate of 0.00057 $m^3/s/m^2$ (surface area) [37], about 0.4 ACH for the testbed. 0.7 and 0.18 ACHs are selected based on the practical building operation considering ASHRAE 90.1 2004 infiltration rate assumption with two exposed walls facing South and North.

Figure 4 Experiment cell space with an office configuration representing light internal thermal mass

Figure 5 Experiment cell with about 1000 added books representing heavy internal thermal mass

A designated fan was installed to control the amount of exhaust air, which could introduce the same amount of outdoor air through the supply duct with an open damper and the door and window gap. This makes the internal space pressure negative; thus the equal amount of exhaust air be infiltrated through the supply air duct as well as cracks, door, window frame gaps. The controlled experiment measured the amount of the exhaust air amount through for the accurate infiltration airflow calculation. The tracer gas decay method was used to measure the air change per hour in the testing cell. The tracer gas concentration decay method is commonly used to calculate the air change rate under conditions of less than 10 ACH. The tracer gas (CO_2) was injected into the testbed cell for a short period of time until the equilibrium concentration level is achieved, i.e., the room air was well mixed. The tracer gas concentration was measured at one-minute interval. As the decay of the tracer gas concentration includes old air as well as a certain amount of fresh air from infiltration, the logarithmic equations introduced in [38–40] were used to calculate ACH from a correlation between the tracer gas concentration and the time. Figure 6 shows (a) the tracer gas release using a CO_2 gas tank, (b) the CO_2 concentration level from the equilibrium status to a full decay showing the exponential curve, and (c) the calculated ACH, for example, 2.0 for the high infiltration scenario.
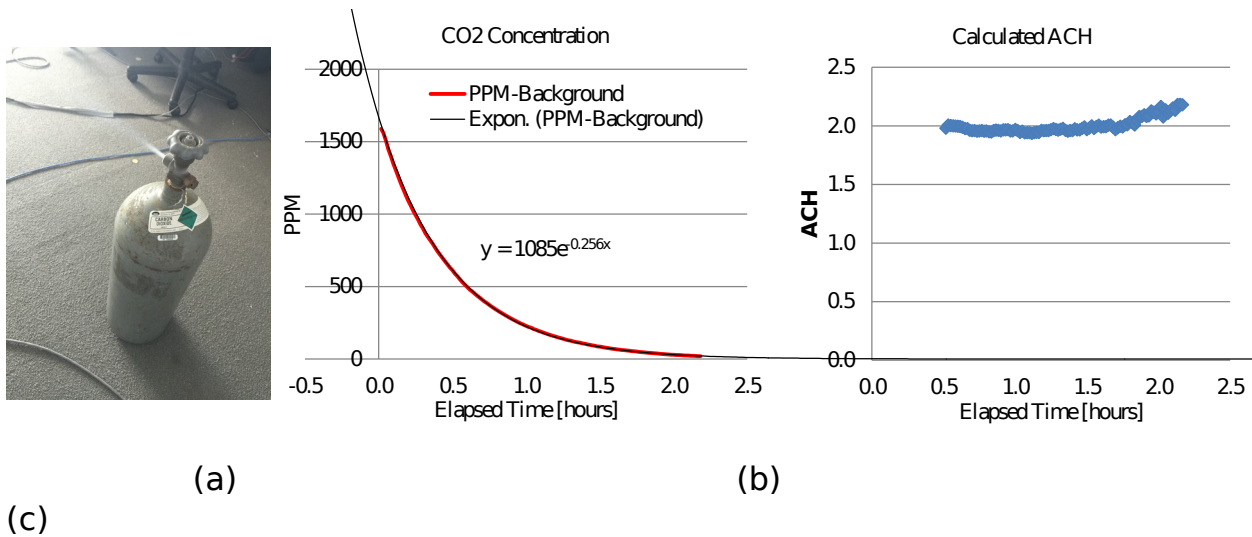
CO2 Concentration

$y = 1085e^{0.256x}$

Calculated ACH

(a) (b)

(c)

Figure 6 ACH measurement using CO_2 tracer gas. (a) CO_2 gas release, (b) CO_2 concentration in the testbed, and (c) Calculated 2.0 ACH for the high infiltration scenario

Figure 7 shows infrared images of the experimental cell under the high infiltration level of 2.0 ACH at 1 pm, which illustrates the significance of the infiltration for the zone air heat balance. The image (a) shows that window frames introduce unwanted cold air into the cell. The image (b) shows significant heat transfer from the direct infiltration through gaps in the entrance door and mechanical system closet door. The infiltration is an unknown and hard-to-get input to energy modeling unless the tracer gas concentration testing is conducted. The inverse model calculates the overall infiltration rate using the indoor measured temperature.
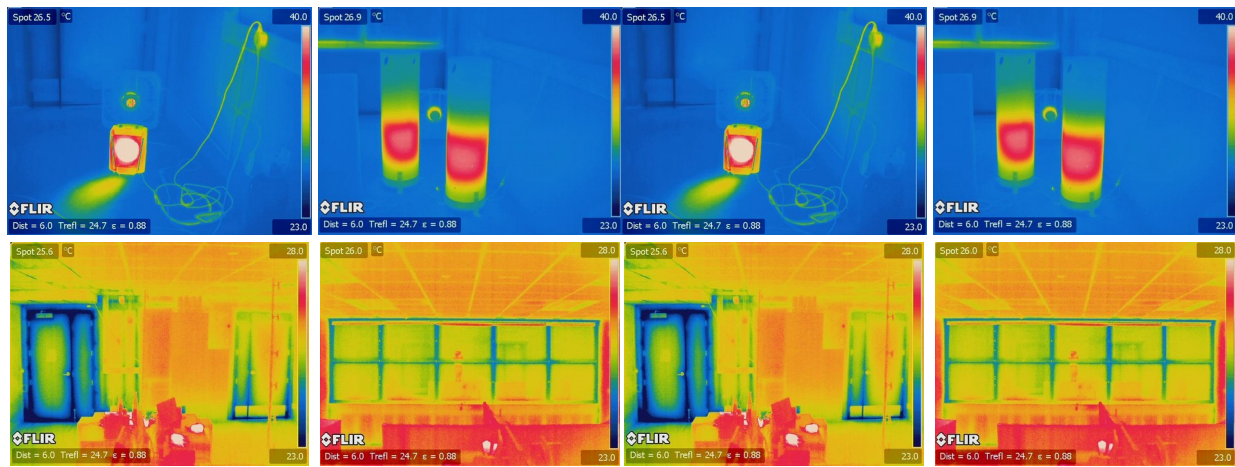
<div align="center">(a)   (b)</div>

Figure 7 Infrared images of window frames (a) and Entrance door and mechanical closet door (b)

The experiment recorded sensor data for energy model development and model validation. The sensor data include:

- Zone air temperature from 28 sensors (four stratification trees, each with seven sensors). The average temperature from the 20 sensors is used as the zone air temperature data. The top (underneath the ceiling tile) and bottom (above the floor) temperature sensors from each stratification tree were excluded from the average calculation

- Electric power from individual outlets for electric heaters, air mixing fans, exhaust air fan, and control systems (computers, sensor connection hubs).

- CO_2 PPM decay data for each zone infiltration case

- Outside air inlet temperature from the supply air duct

- Internal wall surface and slab temperature

- Outdoor air dry-bulb temperature, global solar irradiation, diffuse solar radiation, and wind speed

3. EnergyPlus model for the inverse model validation

An EnergyPlus model that represents the FLEXLAB testbed cell was developed to validate the results from the inverse model against the measured data from the experiment. Figure 8 shows screenshots of the Testbed 3 EnergyPlus model. The developed EnergyPlus model reflects the physical properties of the testbed structure, real measurement of internal heat gain, and outdoor airflow designed to simulate free-floating zone air temperature. FLEXLAB measures local climate data including the outdoor air dry-bulb temperature, the global solar irradiation, the diffuse solar radiation, and the wind speed and direction, which were compiled into EnergyPlus weather (epw) file for the simulation using the actual outdoor environment.
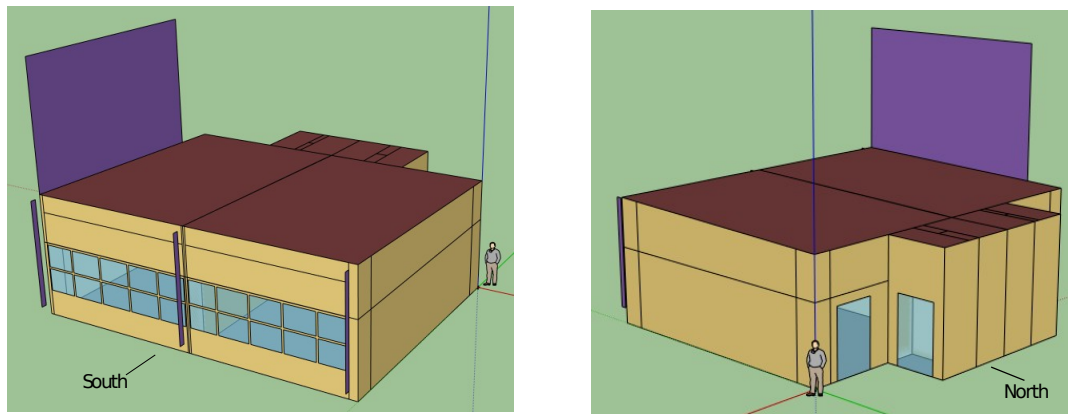

Figure 8 Schematic view of the EnergyPlus model for the FLEXLAB Testbed 3

To capture these internal mass for the light internal thermal mass and the heavy mass configuration with 1000 library books in 50 boxes, we used forward EnergyPlus simulations to empirically determine the zone capacitance multipliers corresponding to these two configurations. The internal mass multiplier was set to 3.0 and 5.0 representing the best for the light and heavy internal thermal mass respectively from the FLEXLAB EnergyPlus simulations. The initial EnergyPlus model has an internal mass multiplier of 1.0, which represents no internal mass object. We iteratively tested different multipliers to find the best multipliers representing the internal mass of the experiment design for the light mass and the heavy mass with books of typical office settings. Normalized Mean Bias Error (NMBE) and Coefficient of Variance of Root Mean Square Error (CVRMSE) are commonly used, as defined in ASHRAE 14 Guideline, to determine the goodness of fit between the simulation results and the measured data [41].

$$NMBE = \frac{\sum_{i=1}^{n}(y_i - ¿\hat{y}_i)}{\acute{y} \times n} \times 100 ¿$$

$$CVRMSE = ¿¿¿$$

Where y represents the simulation temperature, $\hat{y}$ for the measured temperature, ȳ for the mean of the simulated temperature, n for the number of data points. Two sets of results, simulated and measured temperature show that the NMBE and CVRMSE are no greater than 2% for the 10-minute timestep results as shown in Table 2, which indicates the EnergyPlus model well represents the experiment conditions.

Table 2 Zone Air Temperature from the Calibrated EnergyPlus Model Compared to the Measured Air Temperature

	IM0-INF0	IM0-INF1	IM0-INF2	IM0-INF3	IM1-INF0	IM1-INF1	IM1-INF2	IM1-INF3
NMBE	0.50%	-0.03%	0.13%	-0.33%	0.12%	0.10%	0.68%	-0.26%
CVRMSE	0.85%	0.99%	1.20%	0.82%	1.45%	1.11%	1.50%	1.08%

When conducting an energy performance analysis of the existing buildings for retrofit projects, energy model calibration is one of the critical tasks. The calibration of the forward physics-based energy simulation models involves thousands of input parameters, which yields multiple non-unique solutions [14,42,43]. The conventional calibration uses an unmodified simulation engine and multiple runs to tune multiple input parameters. As a result, mathematical and statistical methods have been of interest in calibration research for automated calibrated building energy models [44,45]. The inverse modeling enables calibrating a building energy model that combines inverse and forward physics-based calculations and essentially performs targeted calibration on specific inputs. The targeted

calibration uses the inverse zone air heat balance algorithms to calculate infiltration and internal thermal mass, while in traditional model calibration, users rely on rules-of-thumb or default values provided by the simulation software. Figure 9 illustrates the concept of calibration using the inverse model. The inverse modeling approach uses a single run of the simulation engine to tune selected parameters to derive the target input parameters and input them in the regular energy models. The EnergyPlus object implemented in 8.7, *HybridModel:Zone*, enables the inverse model simulation triggered by the input flag of "Calculate Zone Air Infiltration Rate" or "Calculate Zone Internal Thermal Mass." Then, the derived values, i.e., the calibrated values from the inverse simulation, are added to the forward model; this offers a more advanced calibration of energy models for existing buildings.
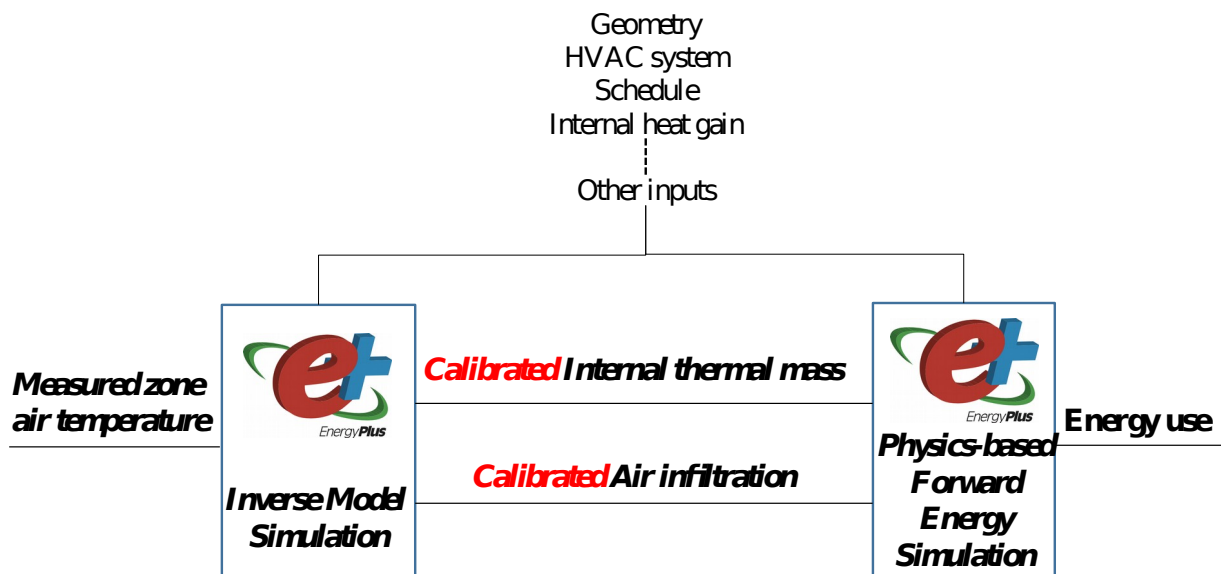

Figure 9 The calibration workflow that integrates the inverse and forward modeling

4. Inverse model validation

The FLEXLAB experiment measured the zone air temperature for three days for each scenario. It is important to consider sufficient time for the indoor air temperature to stabilize due to interactions of the cell structure with the dynamic environmental conditions when calculating the internal mass using the inverse model. Zone air heat capacity needs to be derived from the stabilized internal zone air temperature data that fully captures the stored heat in the air and the internal thermal mass. As discussed in the previous paper [1] that describes the derivation of the inverse model algorithm, an underlying assumption of the inverse model is that the zone heat capacity is treated as constant for the equilibrium of the inversed zone air heat balance model. However, in a mathematical point of view, the calculated heat capacity of zone air and internal thermal mass will vary with the actual dynamic conditions, leading to the varying internal mass multiplier values for different time steps. The inverse model determines a time span that the zone air temperature difference between two adjacent time steps are large enough, to avoid the anomaly or overflow results due to the division term of the inverse model. The inverse model derived more reliable infiltration rates for time steps when the difference between the indoor zone air and outdoor air temperature is greater than 5°C. Considering this, it is recommended that the zone air temperature needs to be measured for at least one week to ensure we have adequate time periods of needed

measured data. However, in our experiments, measured temperature data was limited to three days for each case. To overcome this limitation, four days of simulated temperature data, from the calibrated model, were added to the dataset. Such seven days of the zone air temperature data were then used to derive the infiltration airflow rate and internal mass multiplier under the inverse model simulation mode.

Table 3 shows the summary of the inverse modeling results that used the measured zone air temperature for each test case. The table presents the average calculated infiltration and internal mass multipliers. Further details of the inverse modeling results are presented in Figure 10 for the low internal mass case (IM0) with the infiltration airflow rate 0.42 ACH case (INF1) and in Figure 11 for the heavy internal mass case (IM1) with the scheduled infiltration (INF3). Each chart includes the calculated infiltration airflow rate converted to ACH and the internal mass multipliers at each timestep. The rectangular box in the chart indicates three days of the inverse simulation using the real measured zone air temperature. There are noises in the calculated infiltration airflow rates and internal mass multipliers for the period when the measured zone air temperature data were used. Although the energy model reflects the dynamics of the indoor environment, differences in the zone air temperature add uncertainties to the model parameters.

Table 3 The Calculated Infiltration and Internal Mass Multiplier using the Measured Zone Air Temperature

	Infiltration ACH			Internal Mass Multiplier		
	EnergyPlus input	Inverse modeling results		EnergyPlus input	Inverse modeling results	
		1 week average	3 days average		1 week average	3 days average
IM0-INF0	0.10	0.11	0.13	3.00	3.24	3.33
IM0-INF1	0.42	0.42	0.42	3.00	3.32	3.53
IM0-INF2	2.00	1.97	1.93	3.00	3.92	4.53
IM0-INF3	0.7 nighttime, 0.18 daytime	0.69 nighttime, 0.18 daytime	0.66 nighttime, 0.19 daytime	3.00	3.17	3.23
IM1-INF0	0.10	0.10	0.10	5.00	4.90	3.60
IM1-INF1	0.42	0.42	0.42	5.00	4.99	4.04
IM1-INF2	2.00	2.02	2.05	5.00	5.70	5.98
IM1-INF3	0.7 nighttime, 0.18 daytime	0.65 nighttime, 0.19 daytime	0.7 nighttime, 0.17 daytime	5.00	5.07	4.20

IM0-INF1 Experiment

IM1-INF3 Experiment

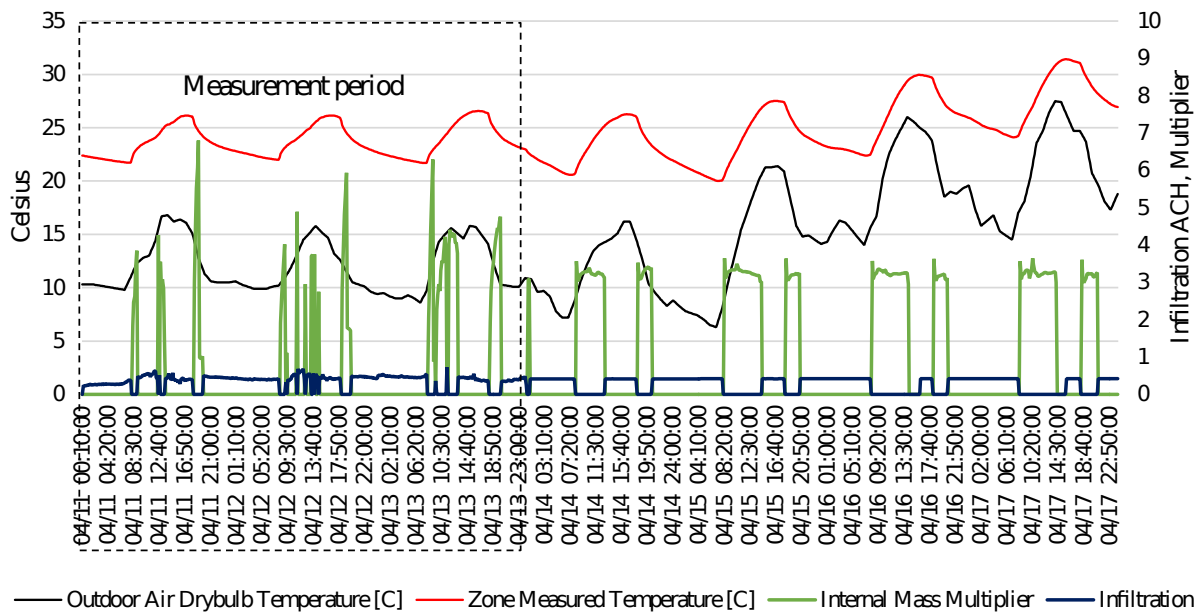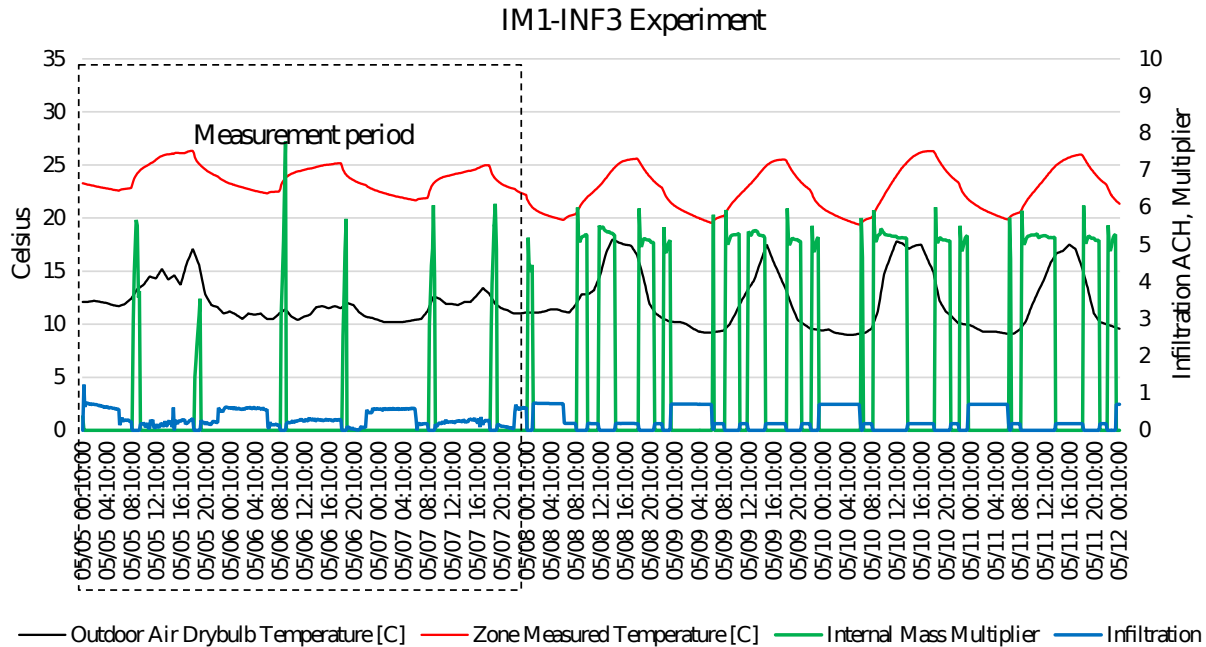Figure 11 The Calculated Infiltration and Internal Mass Multiplier for the IM1-INF3 Experiment Case using the Measured Zone Air Temperature

An underlying assumption is that the zone heat capacity is treated as a constant variable for the equilibrium in the inversed zone air heat balance model. However, it should be noted that the calculated internal thermal mass multiplier varies with dynamic conditions, leading to the varying multipliers *i*n a mathematical point of view. The internal mass multiplier calculations are only done when the zone air temperature differences for two adjacent time steps are greater than 0. This avoids the anomaly or overflow results from incorrect use of the inverse model. The inverse equation derives more reliable infiltration flowrates for time steps when the difference

between the indoor zone air and outdoor air temperature is greater than 5°C [1]. Figure 10 and Figure 11 show timesteps that the inverse simulation was able to calculate internal mass multipliers and infiltration ACH values.

The validation using the FLEXLAB experiment data enlightened the guideline on how to use the inverse model implemented in EnergyPlus. The internal thermal mass is an important component for building performance as it stabilizes internal temperature. Thus a certain period of the measured zone air temperature is needed to capture the thermal inertia of the building structure and interior furnishing equipment. It is recommended to measure the zone air temperature for at least seven days.

The accuracy of the inverse model is dependent on the completeness of the energy model. The infiltration airflow rate and internal mass multipliers are inversely derived using the energy model with the new input of measured air temperature data. Thus, other uncertain parameters will have impacts on the infiltration and internal mass multipliers, because there are multiple combinations of the parameter values that can lead to the environmental condition of the measured zone air temperature. The actual weather data is also needed for the period of the inverse simulation. Future research is needed to investigate how the inverse model can be integrated with the traditional model calibration process to improve the accuracy of the simulation.

The current implementation of the inverse model applies to operation periods when HVAC systems are off, i.e., spaces are in a free-floating mode.

However, this is not a limitation of the inverse model but rather based on the assumption that measured energy delivered by HVAC systems (from the air side or water side of the coil) is not easily available in practice. When the measured energy at timestep from the HVAC systems (delivered energy or supply airflow and temperature) is known, the inverse model also applies.

5. Conclusions

This paper provides details of the validation method and the results of the inverse model using the data collected from the controlled experiments conducted at FLEXLAB. The experiments were designed to collect zone air temperature data under eight controlled testing configurations including two internal mass levels and four infiltration airflow rates. The measured zone air temperature was used to inversely calculate the internal thermal mass multipliers and infiltration airflows for each validation scenario using the inverse model feature implemented in EnergyPlus. The inverse model simulation results show good agreements with the measured data from the FLEXLAB experiments. Insights learned from the validation using the FLEXLAB experiments inform the application of the inverse model. It is expected that the inverse model implemented in EnergyPlus enables more accurate energy performance predictions to inform energy-efficiency retrofit decision making for existing buildings.

A limitation is noted on the use of the combined 3-day measured data and the 4-day simulation data for the validation. Ideally, a seven-day or longer period of measured data would be needed for a cleaner validation, which is a

future work when the dataset is available. The inverse model is not intended to replace the traditional energy model calibration methods. Instead its use in combination with the traditional energy model calibration methods would provide the optimal benefit, which will be described in a future publication.

Acknowledgment

References

[1]   T. Hong, S.H. Lee, Integrating physics-based models with sensor data : An inverse modeling approach, Build. Environ. 154 (2019) 23–31. doi:10.1016/j.buildenv.2019.03.006.

[2]   J.A. Clarke, Energy Simulation in Building Design 2nd Edition, Butterworth-Heinemann, 2001.

[3]   B.D. Hunn, Fundamentals of Building Energy Dynamics, MIT Press, 1996.

[4]   DOE, EnergyPlus Engineering Reference: The Reference to EnergyPlus Calculations, 2015.

[5]   ISO, ISO 13790: 2008 Energy performance of buildings —Calculation of energy use for spaceheating and cooling, (2008).

[6]   W.J. Cole, K.M. Powell, E.T. Hale, T.F. Edgar, Reduced-order residential home modeling for model predictive control, Energy Build. 74 (2014) 69–77.

[7]   G. Kokogiannakis, P. Strachan, J. Clarke, Comparison of the simplified

methods of the ISO 13790 standard and detailed modelling programs in a regulatory context, J. Build. Perform. Simul. 1 (2008) 209–219.

[8] T. Hong, S.. Chou, T.. Bong, Building simulation: an overview of developments and information sources, Build. Environ. 35 (2000) 347–361.

[9] G. Augenbroe, Trends in building simulation, Build. Environ. 37 (2002) 891–902. doi:10.1016/S0360-1323(02)00041-0.

[10] H.X. Zhao, F. Magoulès, A review on the prediction of building energy consumption, Renew. Sustain. Energy Rev. 16 (2012) 3586–3592.

[11] D.B. Crawley, J.W. Hand, M. Kummert, B.T. Griffith, Contrasting the capabilities of building energy performance simulation programs, Build. Environ. 43 (2008) 661–673.

[12] S.H. Lee, T. Hong, M.A. Piette, S.C. Taylor-Lange, Energy retrofit analysis toolkits for commercial buildings: A review, Energy. 89 (2015) 1087–1100. doi:10.1016/j.energy.2015.06.112.

[13] S.H. Lee, T. Hong, M.A. Piette, G. Sawaya, Y. Chen, S.C. Taylor-Lange, Accelerating the energy retrofit of commercial buildings using a database of energy efficiency performance, Energy. 90 (2015) 738–747.

[14] Y. Heo, R. Choudhary, G. Augenbroe, Calibration of building energy models for retrofit analysis under uncertainty, Energy Build. 47 (2012) 550–560.

[15] T. Hong, M.A. Piette, Y. Chen, S.H. Lee, S.C. Taylor-Lange, R. Zhang, K. Sun, P. Price, Commercial Building Energy Saver: An energy retrofit analysis toolkit, Appl. Energy. 159 (2015) 298–309.

[16] S. Verbeke, A. Audenaert, Thermal inertia in buildings: A review of impacts across climate and building use, Renew. Sustain. Energy Rev. 82 (2018) 2300–2318. doi:10.1016/j.rser.2017.08.083.

[17] H. Johra, P. Heiselberg, Influence of internal thermal mass on the indoor thermal dynamics and integration of phase change materials in furniture for building energy storage: A review, Renew. Sustain. Energy Rev. 69 (2017) 19–32. doi:10.1016/j.rser.2016.11.145.

[18] R. Zeng, X. Wang, H. Di, F. Jiang, Y. Zhang, New concepts and approach for developing energy efficient buildings: Ideal specific heat for building internal thermal mass, Energy Build. 43 (2011) 1081–1090.

[19] S. Wang, X. Xu, Parameter estimation of internal thermal mass of building dynamic models using genetic algorithm, Energy Convers. Manag. 47 (2006) 1927–1941.

[20] G. Han, J. Srebric, E. Enache-Pommer, Different modeling strategies of infiltration rates for an office building to improve accuracy of building energy simulations, Energy Build. 86 (2015) 288–295.

doi:10.1016/j.enbuild.2014.10.028.

[21] K. Gowri, D. Winiarski, R. Jarnagin, PNNL-18898: Infiltration Modeling Guidelines for Commercial Building Energy Analysis, PNNL, 2009.

[22] J.K. Kissock, J.S. Haberl, D.E. Claridge, Development of a Toolkit for Calculating Linear, Change-Point Linear and Multiple-Linear Inverse Building Energy Analysis Models, ASHRAE Research Project 1050-RP, Final Report. Energy Systems Laboratory, Texas A&M University, 2002.

[23] DOE, EnergyPlus, (2016). https://energyplus.net/ (accessed May 18, 2016).

[24] IEA, IEA EBC Annex 58 DYNASTEE: DYNamic Analysis. Simulation and Testing applied to the Energy and Environmental performance of buildings, (2014).

[25] LBNL, FLEXLAB The World's Most Advanced Building Efficiency Test Bed, (2016). https://flexlab.lbl.gov/.

[26] A. McNeil, C. Kohler, E.S. Lee, S. Selkowitz, High Performance Building Mockup in FLEXLAB, 2014. doi:LBNL-1005151.

[27] E.S. Lee, D. Geisler-Moroder, G. Ward, Modeling the direct sun component in buildings using matrix algebraic approaches: Methods and validation, Sol. Energy. 160 (2018) 380–395. doi:10.1016/j.solener.2017.12.029.

[28] H. Tang, P. Raftery, X. Liu, S. Schiavon, J. Woolley, F.S. Bauman, Performance analysis of pulsed flow control method for radiant slab system, Build. Environ. 127 (2018) 107–119. doi:10.1016/j.buildenv.2017.11.004.

[29] J. Pantelic, S. Schiavon, B. Ning, E. Burdakis, P. Raftery, F. Bauman, Full scale laboratory experiment on the cooling capacity of a radiant floor system, Energy Build. 170 (2018) 134–144. doi:10.1016/j.enbuild.2018.03.002.

[30] J. Pantelic, F. Bauman, P. Raftery, S. Schiavon, J. Woolley, Side-by-side laboratory comparison of space heat extraction rates and thermal energy use for radiant and all-air systems, Energy Build. 176 (2018) 139–150. doi:10.1016/j.enbuild.2018.06.018.

[31] C. Regnier, P. Mathew, D. Ph, A. Robinson, P. Schwartz, J. Shackelford, T. Walter, D. Ph, Beyond Widgets : Validated Systems Energy Savings and Utility Custom Incentive Program Systems Trends Packaged Integrated Systems : Validated Energy Savings, in: 2018 ACEEE Summer Study Energy Effic. Build., 2018: pp. 1–12.

[32] Philip Haves, Validation and Uncertainty Characterization for Energy Simulation, in: US DOE 2017 Build. Technol. Off. Peer Rev., 2017.

[33] E. Vrettos, E.C. Kara, J. MacDonald, G. Andersson, D.S. Callaway,

Experimental Demonstration of Frequency Regulation by Commercial Buildings - Part II: Results and Performance Evaluation, ArXiv:1605.05835. (2016). http://arxiv.org/abs/1605.05558.

[34] C. Regnier, P. Mathew, D. Ph, A. Robinson, P. Schwartz, Beyond Widgets – Systems Incentive Programs for Utilities, 2016. http://eetd.lbl.gov/sites/all/files/1006195.pdf%5Cnhttps://cbs.lbl.gov/sites/all/files/beyond-widgets-ppt-09-2016.pdf.

[35] S. Dawson-Haggerty, X. Jiang, G. Tolle, D.E. Culler, SMAP - A Simple Measurement and Actuation Profile for physical information, in: Proc. 8th Int. Conf. Embed. Networked Sens. Syst. SenSys 2010, Novemb. 3-5, 2010, Zurich, Switzerland, 2010.

[36] M. Deru, K. Field, D. Studer, K. Benne, B. Griffith, P. Torcellini, B. Liu, M. Halverson, D. Winiarski, M. Rosenberg, M. Yazdanian, J. Huang, D. Crawley, U . S . Department of Energy Commercial Reference Building Models of the National Building Stock, 2011.

[37] U.S. DOE, Commercial Prototype Building Models, (2019). https://www.energycodes.gov/development/commercial/prototype_models#90.1 (accessed May 30, 2019).

[38] D. Laussmann, D. Helm, Air Change Measurements Using Tracer Gases: Methods and Results. Significance of air change for indoor air quality, in: N. Mazzeo (Ed.), Chem. Emiss. Control. Radioact. Pollut. Indoor Air Qual., IntechOpen, 2011. doi:http://dx.doi.org/10.5772/57353.

[39] ISO, Thermal Performance of Buildings and Materials – Determination of Specific Airflow Rate in Buildings — Tracer gas Dilution Method, 12569:2012, Geneva, Switzerland, 2012.

[40] ASTM, Standard Test Method for Determining Air Change in a Single Zone by Means of a Tracer Gas Dilution, West Conshohocken, PA, US, 2011.

[41] ASHRAE, ASHRAE Guideline 14-2002: Measurement of Energy and Demand Savings, 2002.

[42] G. Chaudhary, J. New, J. Sanyal, P. Im, Z. O'Neill, V. Garg, Evaluation of "Autotune" calibration against manual calibration of building energy models, Appl. Energy. 182 (2016) 115–134. doi:10.1016/j.apenergy.2016.08.073.

[43] K. Sun, T. Hong, S.C. Taylor-Lange, M.A. Piette, A pattern-based automated approach to building energy model calibration, Appl. Energy. 165 (2016) 214–224. doi:10.1016/j.apenergy.2015.12.026.

[44] J. Mao, Y. Fu, A. Afshari, P.R. Armstrong, L.K. Norford, Optimization-aided calibration of an urban microclimate model under uncertainty, Build. Environ. 143 (2018) 390–403. doi:10.1016/j.buildenv.2018.07.034.

[45] A. Chong, W. Xu, S. Chao, N.T. Ngo, Continuous-time Bayesian calibration of energy models using BIM and energy data, Energy Build. 194 (2019) 177–190. doi:10.1016/j.enbuild.2019.04.017.